Supplementary Material

Reversible small molecule inhibitors of MAO A and MAO B with anilide motifs

Author name: Jens Hagenow,[1] Stefanie Hagenow,[1] Kathrin Grau,[1] Mohammad Khanfar,[1,2,3] Lena Hefke,[4] Ewgenij Proschak,[4] Holger Stark[1,*]

Author affiliations

[1] Heinrich Heine University Düsseldorf, Institute of Pharmaceutical and Medicinal Chemistry, Universitaetsstr. 1, 40225 Duesseldorf, Germany

[2] Faculty of Pharmacy, The University of Jordan, P.O Box 13140, Amman 11942, Jordan

[3] College of Pharmacy, Alfaisal University, Al Takhassusi Rd, Riyadh, 11533, Saudi Arabia.

[4] Goethe University Frankfurt, Institute of Pharmaceutical Chemistry, Max-von-Laue-Str. 9, 60438 Frankfurt, Germany

[*]Corresponding Author

Correspondence: Prof. Dr. Holger Stark

Heinrich Heine University Duesseldorf, Institute of Pharmaceutical and Medicinal Chemistry, Universitaetsstr. 1, 40225 Duesseldorf, Germany

Tel +49 211 81-10478

Fax +49 211 81-13359

Email stark@hhu.de

Molecular Docking

Docking poses of compounds **31**, **33**, **34**, **39**, and **65** within MAO A and B binding pockets.

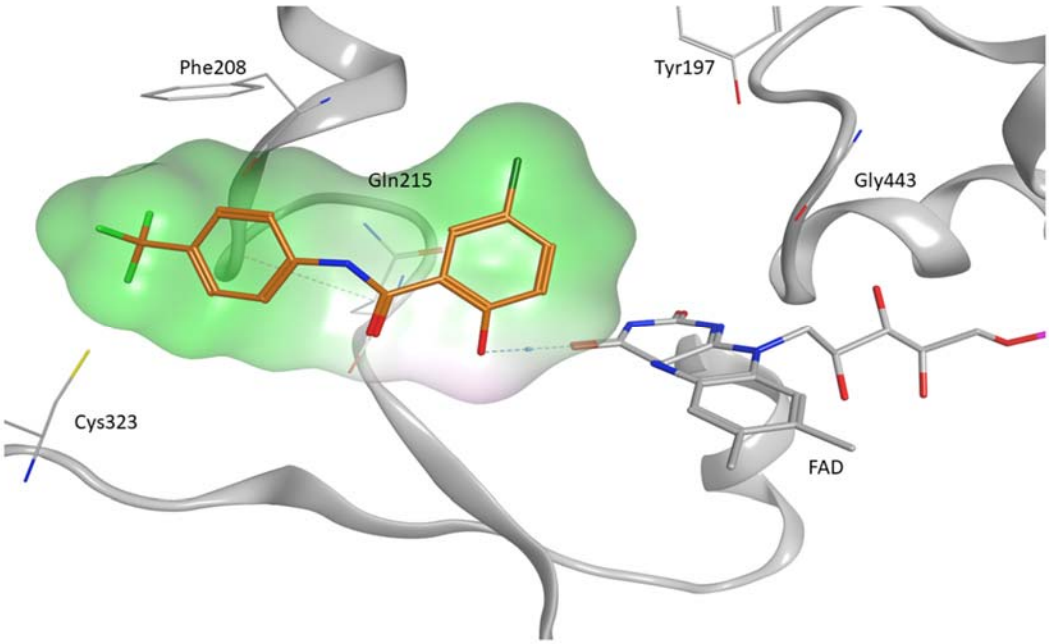

Figure S1 Visualization of **31** in the binding pocket of MAO A.

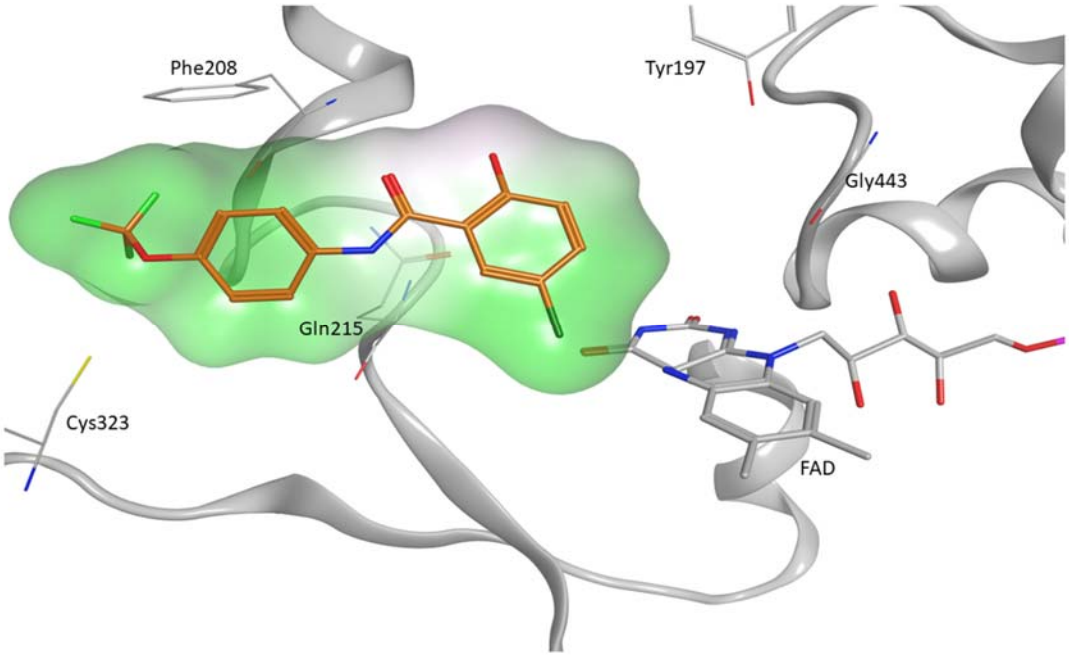

Figure S2 Visualization of **33** in the binding pocket of MAO A.

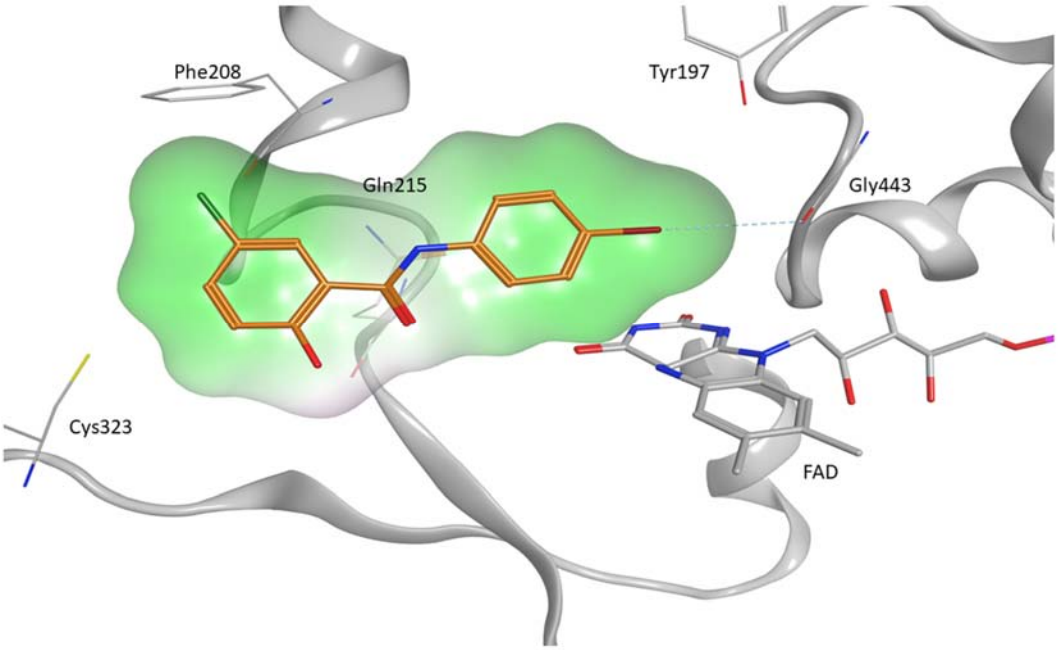

Figure S3 Visualization of **34** in the binding pocket of MAO A.

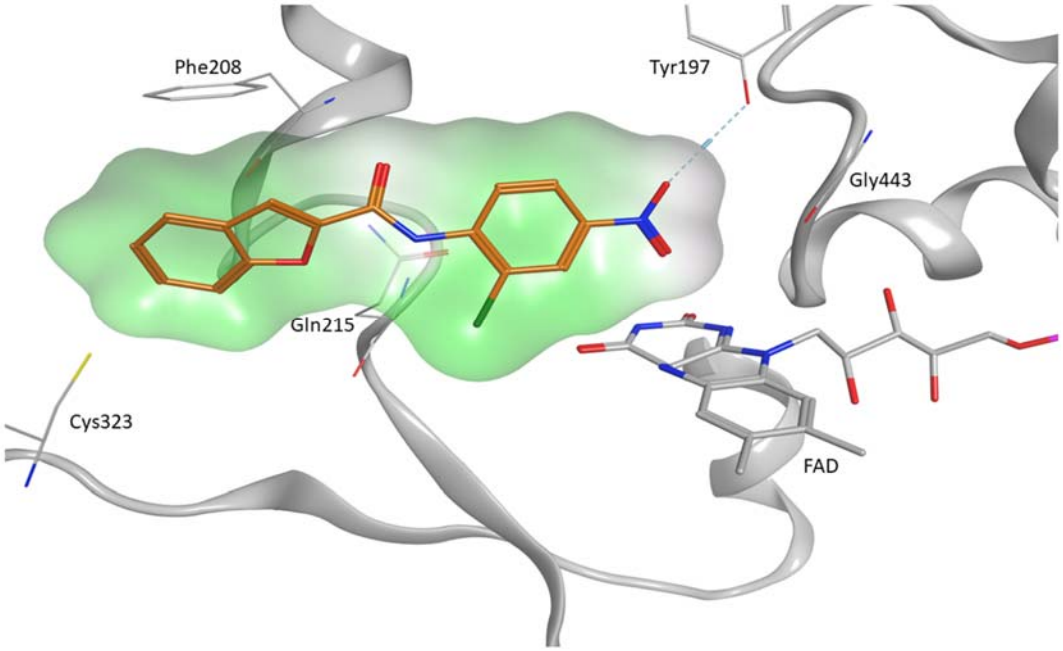

Figure S4 Visualization of **65** in the binding pocket of MAO A.

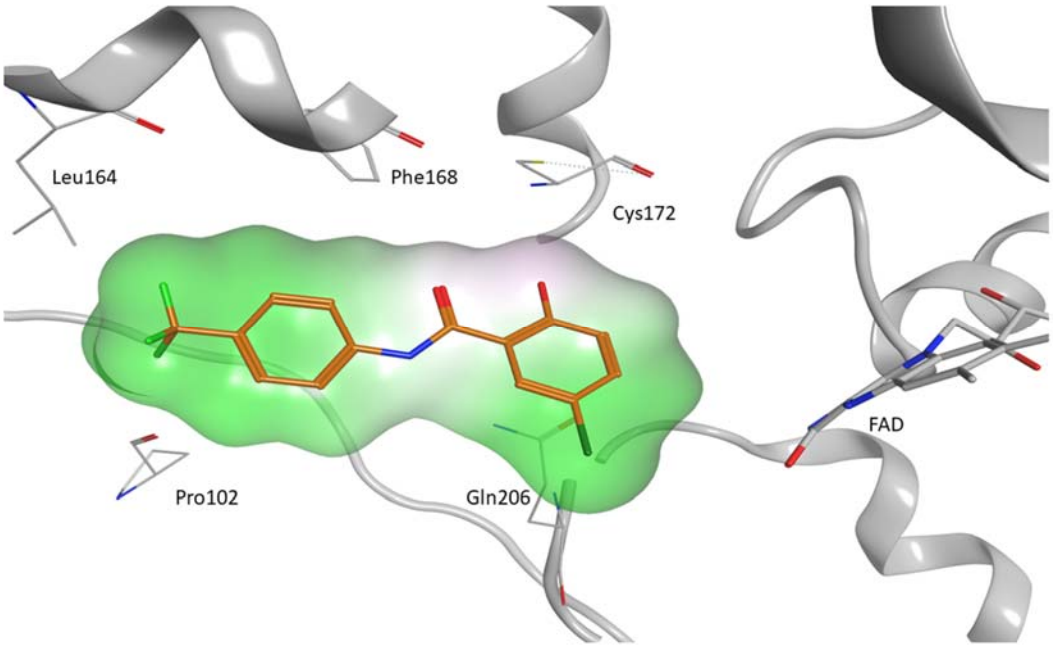

Figure S5 Visualization of **31** in the binding pocket of MAO B.

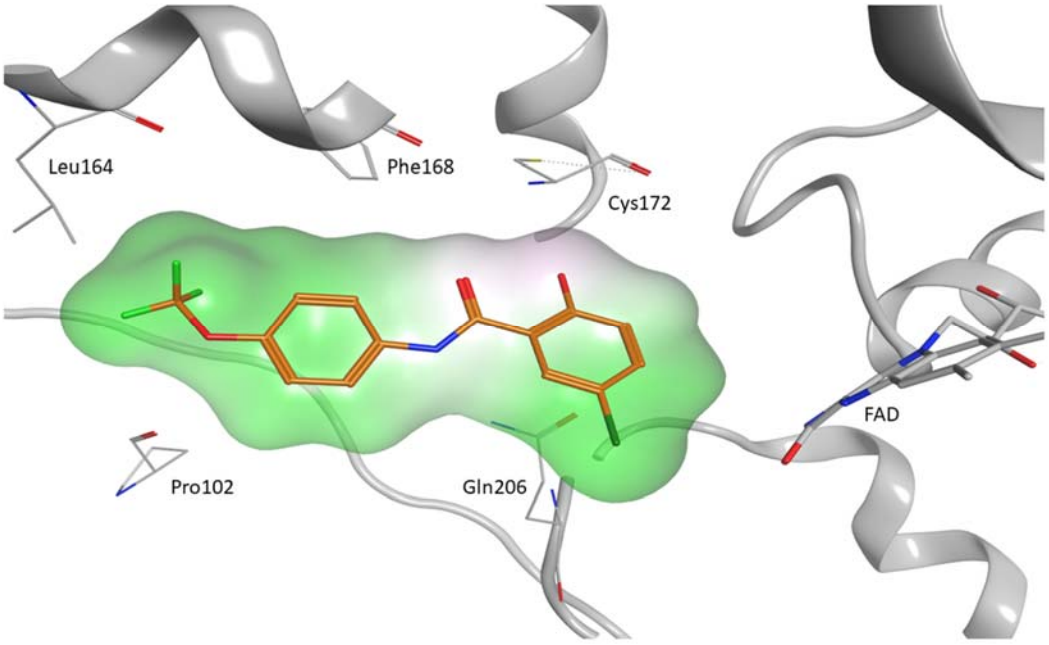

Figure S6 Visualization of **33** in the binding pocket of MAO B.

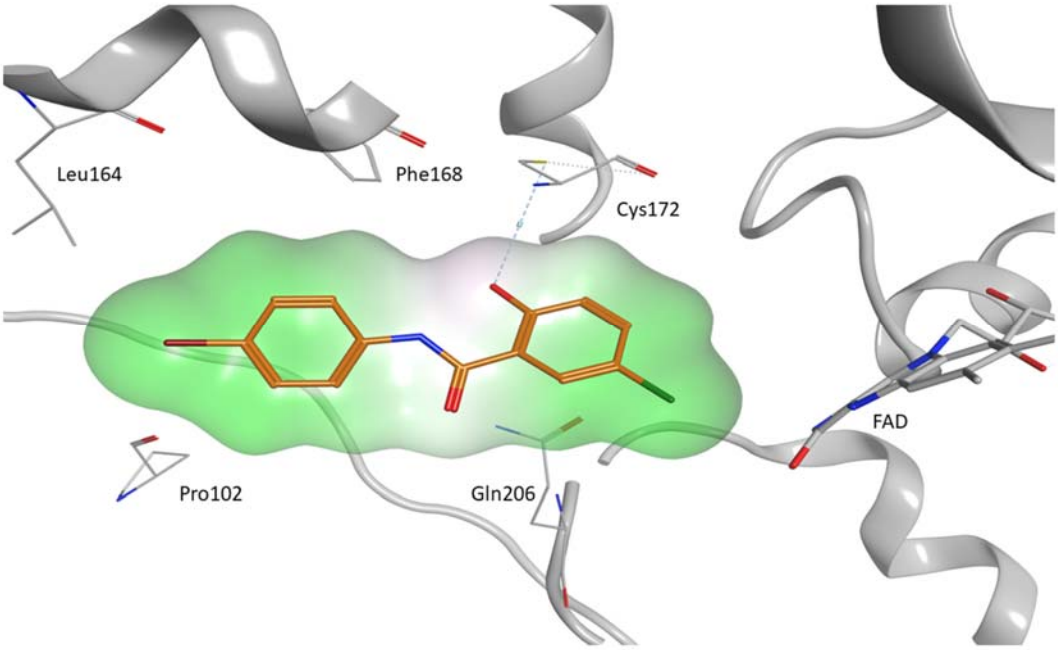

Figure S7 Visualization of **34** in the binding pocket of MAO B.

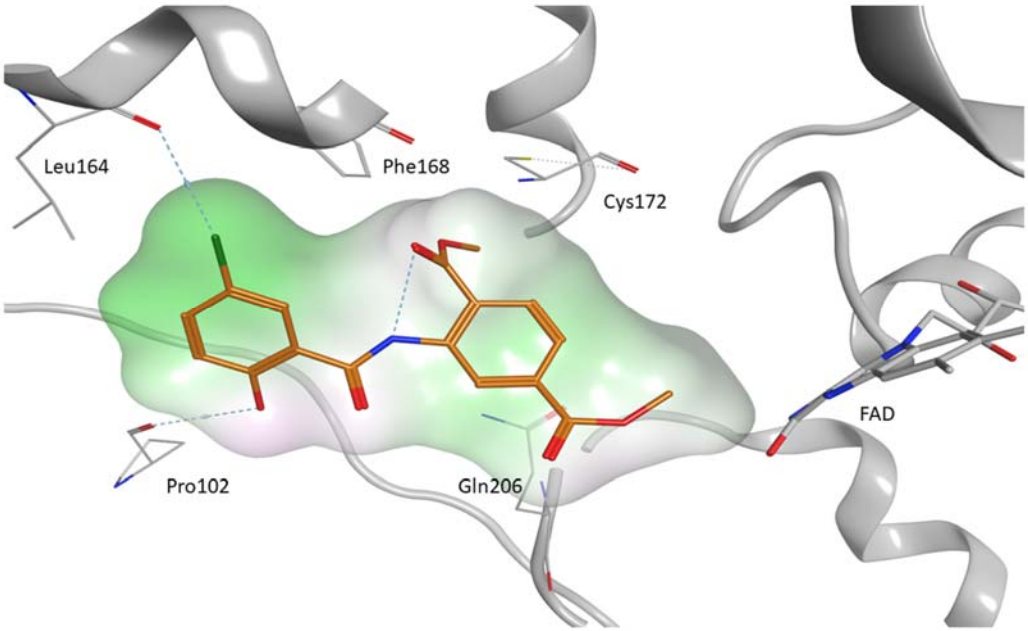

Figure S8 Visualization of **39** in the binding pocket of MAO B.

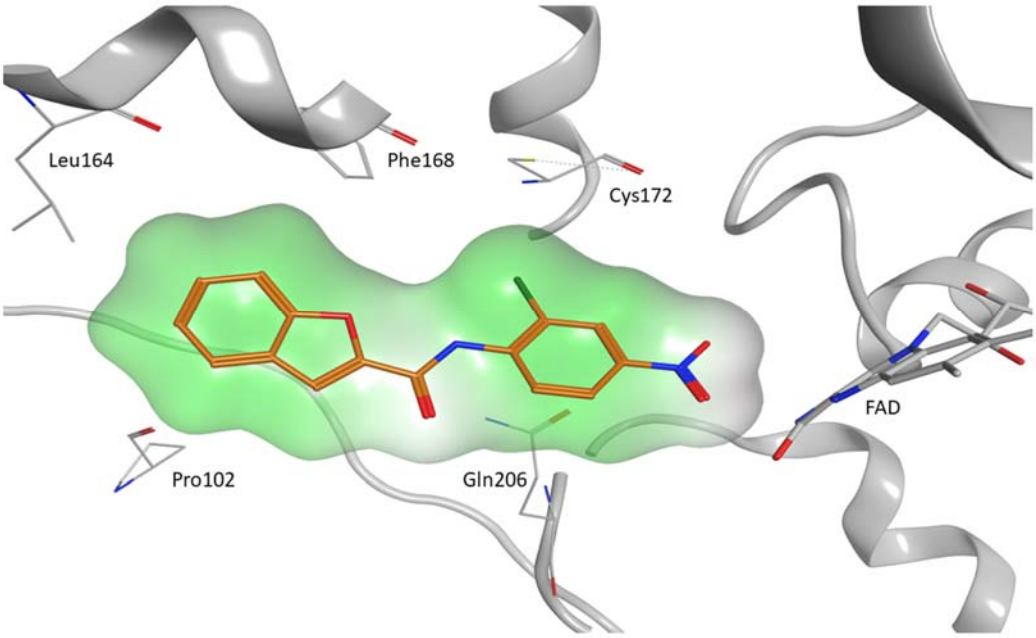

Figure S9 Visualization of **65** in the binding pocket of MAO B.

Pharmacophore Modeling and ROC Analyses

HipHop module of Discovery studio software 2.5.5 was used to construct pharmacophoric hypotheses of MAO-A and MAO-B inhibitors. HipHop works by identifying the three-dimensional arrangements of chemical features that are mutual to active molecules. Principal and MaxOmitFeat parameters define how many compounds must map completely or partially to the pharmacophoric hypothesis. A subset of 25 representative compounds was selected for HipHop run. Table S1 describes the how training compounds were classified into active, moderately active, and inactive compounds.

Active ligands were assigned Principal and MaxOmitFeat values of 2 and 0, respectively, to ensure that all of their chemical features will be considered in building the pharmacophore space. Moderately active compounds were assigned a Principal value of 1 to ensure that they will be mapped at least once by each generated hypothesis, and a MaxOmitFeat value of 1 to allow

missing one feature in any generated model. Inactive compounds were assigned a Principal value of zero and MaxOmitFeat of two.

ROC analysis evaluates the ability of a particular pharmacophore model to classify the compounds in a testing list as actives or inactives. The performance of the considered model is judged based on the area under the curve (AUC) of the corresponding ROC as well as the overall specificity, overall accuracy, overall true positive rate, and overall false positive rate.

It was necessary to perform valid evaluation of structural database (testing set) that consists of an adequate list of decoy compounds in combination with diverse list of known active compounds. The testing set included structurally diverse active inhibitors of 14 MAO A and 18 MAO B.[1–3] The decoy list was selected as depicted by Verdonk and co-workers.[4] Briefly, the decoy compounds were prepared relying on three basic one-dimensional (1D) characteristics that permit the estimation of distance (D) between two molecules (e.g., i and j), namely: (1) the number of hydrogen-bond donors (NumHBD); (2) number of hydrogen-bond acceptors (NumHBA) and (3) the number of nonpolar atoms (NP, known as the summation of Cl, F, Br, I, S and C atoms in a particular molecule).

For each active compound in the testing set, the distance to the nearest other active compound is detected using their Euclidean Distance (equation A):

$$D(i,j) = \sqrt{(NumHBD_i - NumHBD_j)^2 + (NumHBA_i - NumHBA_j)^2 + (NP_i - NP_j)^2} \qquad \text{(A)}$$

The minimum distances are averaged by calculating the mean over all active compounds (Dmin). After that, for each active molecule in the testing set an average of 36 decoys were chosen in random way from the ZINC database. The decoys were selected in such a pattern that they did not exceed Dmin distance from their corresponding active members.

Additionally, to further diversify the actives compounds, i.e., to prevent close likeness among active compounds in the testing set, any active compound having zero distance D(i,j) from other active compound(s) in the testing set was eliminated. Active testing molecules were defined as those possessing MAO-A and MAO-B inhibitors affinities ≤ 300 nM. The MAO-A testing set

included 14 active compounds and 504 ZINC inactive compounds, while MAO-B testing set included 16 active compounds and 576 ZINC inactive compounds.

The decoy sets were screened by each pharmacophore for ROC curve analysis utilizing the "Best flexible search" option carried out in HYPOGEN, while the conformational spaces of the compounds were formed using the "Fast conformation generation option" applied in HYPOGEN. Compounds that are lacking one or more features were excluded from hit lists. Moreover, decoy set compounds were fitted against the selected pharmacophore and their fit values (best fit values) was determined by equation (B):

$$Fit = \Sigma\ mapped\ hypothesis\ features\ x\ W\ [1 - \Sigma(disp/tol)2] \quad \text{(B)}$$

ROC curves for corresponding pharmacophores were constructed using the hit lists. ROC curve analysis prescribes the sensitivity (Se or true positive rate, Equation C) for any probable change in the number of selected compounds (n) as a function of (1-Sp). Sp is known as specificity or true negative rate (Equation D).

$$Se = \frac{Number of Selected Actives}{Total Number of Actives} = \frac{TP}{TP+FN} \quad \text{(C)}$$

$$Sp = \frac{Number\ of\ Discarded\ Inactives}{Total\ Number\ of\ Inactives} = \frac{TN}{TN+FP} \quad \text{(D)}$$

Where, TP is the number of active compounds that are captured by the virtual screening method (true positives), FN is the number of active compounds ejected by the default screening, TN is the number of excluded decoys (considered inactives), while FP is the number of captured decoys (considered inactives).

A ROC curve is plotted by adjusting the score of the active molecule as the first threshold. After that, the number of decoy compounds within this cut-off is enumerated, and the corresponding Se and Sp pair is detected. This calculation is repeated for the active compound with the second

highest score and so on, until the scores of all actives are represented as a selection of thresholds.

The ROC curve expresses an ideal distribution, where overlapping between the scores of active molecules and decoys does not occur, starts from the origin to the upper-left corner until all the actives are recovered and Se comes the value of 1. Then, the ideal ROC curve keeps as a horizontal straight line to the upper-right corner where all active compounds and all decoy compounds are retrieved, which is indicated by Se = 1 and Sp = 0.

The success of a particular virtual screening workflow can be governed from the following criteria:

1) Area under the ROC curve (AUC): -In a successful ROC curve, an AUC value of 1 is perfect. However, AUC value of 0.5 indicates random distributions. Virtual screening that carries out better than a random recognition of active compounds and decoys retrieve an AUC value between 0.5 and 1.

2) Overall accuracy (ACC): Indicates the percentage of molecules that were classified correctly by the screening protocol (Equation E). Testing compounds are appointed a binary score value of zero (compound captured) or one (compound not captured).

$$ACC = \frac{TP+TN}{N} = \frac{A}{N} x\ Se + \left(1 - \frac{A}{N}\right) xSp \quad \text{(E)}$$

N is the total number of compounds in the testing databaseand A is the number of true active compounds in the testing database.

3) Overall specificity (SPC): Indicates the percentage of excluded inactive compounds by the particular virtual screening workflow. Inactive test compounds are appointed a binary score value of zero (compound captured) or one (compound not captured).

4) Overall true positive rate (TPR or overall sensitivity): Describes the fraction percentage of captured active compounds from the total number of active compounds. Active test compounds are assigned a binary score value of zero (compound captured) or one (compound not captured).

5) Overall false negative rate (FNR or overall percentage of excluded actives): Describes the fraction percentage of active compounds that were excluded by the virtual screening method.

Discarded active test compounds are assigned a binary score value of zero (compound captured) or one (compound not captured).

Table S1 The training subsets employed in exploring the pharmacophoric space of MAO-A and MAO-B inhibitors

Training set	Active[a]	Moderately active[b]	Inactive[c]
MAO-A	**7, 31, 64**	**9, 11, 14, 19, 24, 25, 33, 39, 44, 47, 53, 55, 65**	**17, 36, 42, 43, 50, 59, 60, 63, 66**
MAO-B	**11, 31, 33, 36, 39, 53, 55**	**7, 14, 17, 24, 42, 47, 50, 59, 60, 63, 64, 65, 66**	**9, 19, 25, 43, 44**

Notes: [a]Active MOA-A inhibitors are defined for compounds with IC_{50} value ≤ 300 nM; [b]moderately active inhibitors are defined for compounds that have % of inhibition (at 1 μM) less than 90 % and more than 10 % for MAO-A, and less than 80 % and more than 10 % for MAO-B; [c]inactive compounds are those that have % of inhibition less than 10 % (at 1 μM).

Table S2 HipHop run parameters employed for exploring MAO-A and MAO-B pharmacophoric spaces

HipHop Run No.	Selected input features (types and ranges)[a]	Number of pharmacophoric features[b]
1	HBA (1 – 3), HBD (0 – 1), Hbic (0 – 1), RingArom (0 – 3)	4 – 5
2	HBA (1 – 3), HBD (0 – 1), Hbic (0 – 1), RingArom (0 – 3), Exv (0 – 10)	4 – 5
3	HBA (2 – 3), HBD (0 – 1), Hbic (0 – 1), RingArom (0 – 3)	4 – 5
4	HBA (2 – 3), HBD (0 – 1), Hbic (0 – 1), RingArom (0 – 3), Exv (0 – 10)	4 – 5
5	HBA (1 – 3), HBD (0 – 2), Hbic (0 – 1), RingArom (0 – 3)	4 – 5
6	HBA (1 – 3), HBD (0 – 2), Hbic (0 – 1), RingArom (0 – 3), Exv (0 – 10)	4 – 5
7	HBA (2 – 3), HBD (0 – 2), Hbic (0 – 1), RingArom (0 – 3)	4 – 5
8	HBA (2 – 3), HBD (0 – 2), Hbic (0 – 1), RingArom (0 – 3), Exv (0 – 10)	4 – 5
9	HBA (1 – 3), HBD (0 – 1), Hbic (0 – 1), RingArom (0 – 3)	5 – 5
10	HBA (1 – 3), HBD (0 – 1), Hbic (0 – 1), RingArom (0 – 3), Exv (0 – 10)	5 – 5
11	HBA (2 – 3), HBD (0 – 1), Hbic (0 – 1), RingArom (0 – 3)	5 – 5
12	HBA (2 – 3), HBD (0 – 1), Hbic (0 – 1), RingArom (0 – 3), Exv (0 – 10)	5 – 5
13	HBA (1 – 3), HBD (0 – 2), Hbic (0 – 1), RingArom (0 – 3)	5 – 5
14	HBA (1 – 3), HBD (0 – 2), Hbic (0 – 1), RingArom (0 – 3), Exv (0 – 10)	5 – 5
15	HBA (2 – 3), HBD (0 – 2), Hbic (0 – 1), RingArom (0 – 3)	5 – 5
16	HBA (2 – 3), HBD (0 – 2), Hbic (0 – 1), RingArom (0 – 3), Exv (0 – 10)	5 – 5

Notes: [a]HBA: Hydrogen Bond Acceptor, HBD: Hydrogen Bond Donor, RingArom: Ring Aromatic, Hbic: Hydrophobic, Exv: excluded volumes, the allowed ranges of input features are in brackets. [b]Other parameters were set to their default values.

Table S3 ROC performance of the highest ranked models for MAO-A and MAO-B inhibitors

Pharmacophore model	ROC –AUC[a]	ACC[b]	SPC[c]	TPR[d]
MAO-A	0.779	0.570	0.548	0.573
MAO-B	0.750	0.277	0.357	0.489

Notes: [a]AUC: area under the curve, [b]ACC: overall accuracy, [c]SPC: overall specificity, [d]TPR: overall true positive rate.

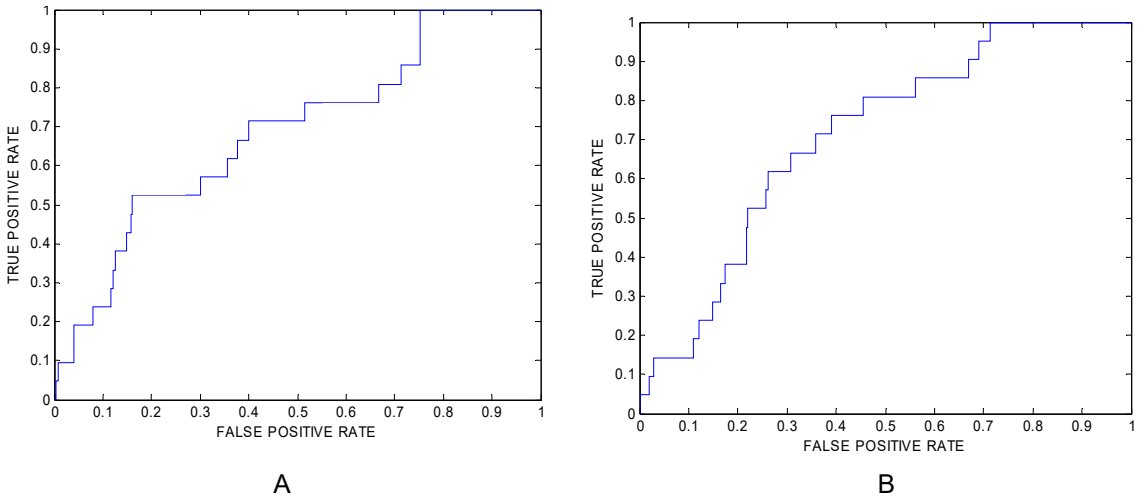

Figure S10 ROC curves of the pharmacophore models of MAO-A and MAO-B, respectively.

Cholinesterase Assays

Cholinesterase inhibition screening was performed according to a modified Ellman's assay.[5,6] Test compounds (10^{-6} and 10^{-5} M) were preincubated with electric eel acetylcholine esterase (eeAChE Type VI-S; 0.0025 U mL^{-1}) or equine serum butyrylcholine esterase (eqBuChE; 0.002 U mL^{-1}) at 37°C for 30 min in a total assay volume of 200 µL (0.1 M potassium phosphate buffer pH 8). The assay was started by adding a solution of dithiobis-nitrobenzoic acid (DTNB; 0.5 mM) and the substrate acetylthiocholine iodide (ATCI; 1 mM) and product formation was monitored

spectrophotometrically (412 nm) at 37°C over a period of 30 min (40 sec intervals). Percentage values were calculated relative to control and physostigmine was used as positive control.

Table S4 AChE and BuChE inhibition rates of ST-2043 (test concentration 10 µM and 1 µM)

	Structure	%Inhibition[a]	
		AChE	**BuChE**
ST-2043	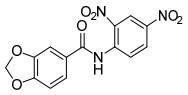	50.7±12.2 (@10 µM) 57.2±4.5 (@1 µM)	34.8±13.0 (@10 µM) 23.7±1.8 (@1 µM)

Notes: [a] Data represent mean values ± standard deviation of four independent experiments each performed in duplicates (global fit). Percentage values were calculated relative to control (set to 100% remained activity).

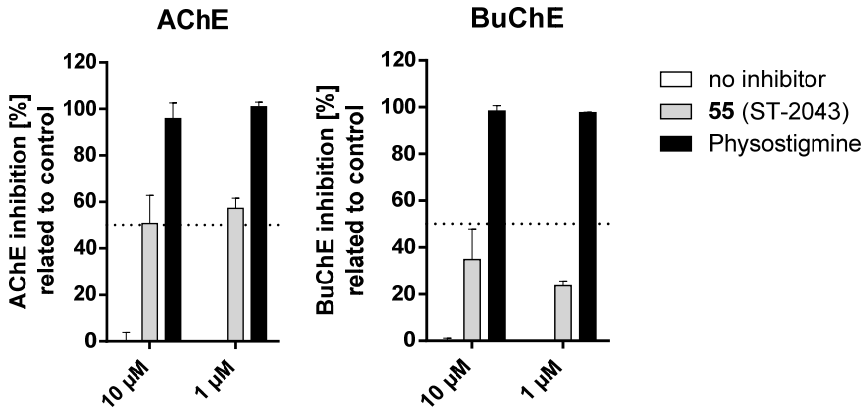

Figure S11 Inhibition of AChE and BuChE after incubation with **55** (ST-2043) and Physostigmine as control. Data represent mean values ± standard deviation of four independent experiments, each performed in duplicates. Percentage values were calculated relative to control (set to 100% remained activity).

MAO B IC_{50} determination

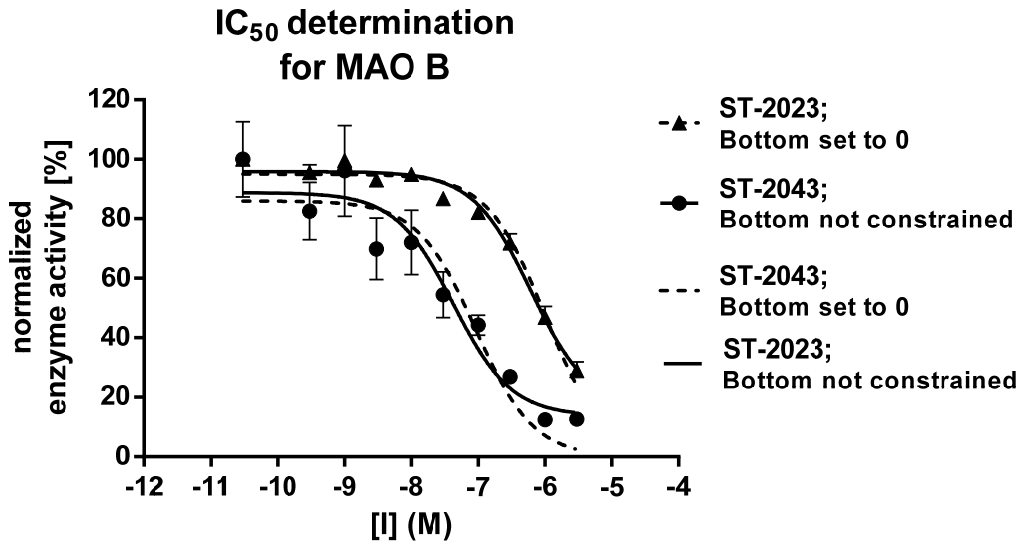

Figure S12 Normalized full inhibition curve for compound **ST-2023** (**7**) and **ST-2043** (**55**) with chosen (Bottom = 0 and Bottom not constrained for **7** and **55**, respectively) and alternative non-linear regression fit mode. Dashed lines represent non-linear fit with bottom plateau set to zero, while solid lines represent a fit with no constrained bottom plateau. Data represent mean values ± standard deviation of four independent experiments, each performed in duplicates.

References

1. Reis J, Cagide F, Chavarria D, et al. Discovery of New Chemical Entities for Old Targets: Insights on the Lead Optimization of Chromone-Based Monoamine Oxidase B (MAO-B) Inhibitors. *J Med Chem*. 2016;59(12):5879-5893.
2. Frédérick R, Dumont W, Ooms F, et al. Synthesis, structural reassignment, and biological activity of type B MAO inhibitors based on the 5H-indeno[1,2-c]pyridazin-5-one core. *J Med Chem*. 2006;49(12):3743-3747.
3. La Regina G, Silvestri R, Artico M, et al. New pyrrole inhibitors of monoamine oxidase: Synthesis, biological evaluation, and structural determinants of MAO-A and MAO-B selectivity. *J Med Chem*. 2007;50(5):922-931.
4. Verdonk ML, Berdini V, Hartshorn MJ, et al. Virtual screening using protein-ligand docking: Avoiding artificial enrichment. *J Chem Inf Comput Sci*. 2004;44(3):793-806.
5. Ellman GL, Courtney KD, Andres V, Featherstone RM. A New an Rapid Colorimetric Determination of Acetylcholinesterase Acivity. *Biochem Pharmacol*. 1961;7:88-95.
6. Ramsay RR, Tipton KF. Assessment of Enzyme Inhibition: A Review with Examples from the Development of Monoamine Oxidase and Cholinesterase Inhibitory Drugs. *Molecules*. 2017;22(7):1192.